A STUDY OF SEISMIC ROAD NOISE

A THESIS

Presented to

The Faculty of the Division of Graduate Studies

by

James Meredith Butler

In Partial Fulfillment

of the Requirements for the Degree

Master of Science in Geophysical Sciences

Georgia Institute of Technoloy

July, 1975

A STUDY OF SEISMIC ROAD NOISE

Approved:

Leland Timothy Long, Chairman

G. Lafayette Maynard

Robert P. Lowell

Date approved by Chairman: 7-21-75

ACKNOWLEDGMENTS

Instrumentation and computer time for this research was provided by the School of Geophysical Sciences, Georgia Institute of Technology. During my tenure as a graduate student, financial support was provided by a research assistant ship in the School of Geophysical Sciences.

Many thanks goes to friends and fellow students, including W. Maitland, M. Maitland, G. Dooley, R. Dooley, C. Speidel, R. Garfield, W. Champion, R. Bridges, and A. Wyatt who helped with field work, general theory, and writing of the thesis.

Drs. L. Maynard and R. Lowell critically read the text.

Dr. L. Long endured helping me through the field work, ideology, and writing of this thesis.

TABLE OF CONTENTS

LIST OF ILLUSTRATIONS

CHAPTER I

INTRODUCTION

Seismic road noise is the ground motion caused by vehicles. Although some seismic road noise is at frequencies greater than 50 Hz, most of the energy is in the frequency range between 2 and 50 Hz. The environmental impact of seismic road noise has been ignored due to much more predominant problems of air, water, and sound pollution. The undesirable effects of seismic road noise are the motions of buildings, especially those of poor construction or in disrepair (this may lead to structural failure) and personal annoyance (1mm./sec. motion can be felt). However, when particle velocity becomes as large as 1mm./sec., the audio frequency vibrations coming through the air are felt strongly also.

The early investigations in high-frequency (1.0 to 100 Hz) seismic ground noise were directed predominantly toward the measurement of the seismic noise from natural sources such as wave motion over water, atmospheric disturbances, landslides, etc. The seismic noise level was related to atmospheric storms or background seismic activity. Later, studies of seismic noise showed that cultural sources such as factories and vehicles were major sources of seismic noise in urban and industrial areas.

Wilson (1953) measured the natural seismic noise level near Cambridge, England. He found the day seismic noise level to be ten to

twenty times the night seismic noise level of 1.5×10^{-6} cm./sec. rms. By comparing data from a geophone near a tree with that from one in a nearby field, he found that the wind moving the tree caused a ground motion of 3×10^{-5} cm/sec. His data were taken in the frequency range between 4 and 100 Hz.

Brune and Oliver (1959) graphed seismic earth surface noise verses period (Figure 1) using data from existing literature. In the frequency range between 1 and 100 Hz, amplitudes of minimum and average seismic noise levels were from 10^{-6} to 10^{-3} and from 10^{-4} to 10^{-2} microns, respectively.

Franti, et al. (1962) analyzed the spectral content in the 0.5 to 31.5 Hz frequency band of seismic noise at locations throughout the U.S. An example of seismic noise spectra in Michigan is shown in Figure 2. An anomalous spectral peak at two Hz was seen in much of the data. Using mathematical analysis involving high-order mode Rayleigh waves, Romney (1953) and Hatherton (1960) could not explain this anomaly. Franti, et al. (1962) found high seismic noise levels on alluvial soil and low noise levels on hard rock. Franti (1963) continued the study to try to correlate spectra to rock type. After extending the frequency range between 0.2 and 100 Hz and using 75 locations throughout the U.S., he found no correlation. Franti attributed the two Hz anomalous peak to either an extreme of group velocity or an unspecified seismic noise source over an extended region (possibly due to traffic and trains). Fix (1972) did spectral work under 10 Hz with similar results.

Train seismic noise in the two to five Hz frequency range was

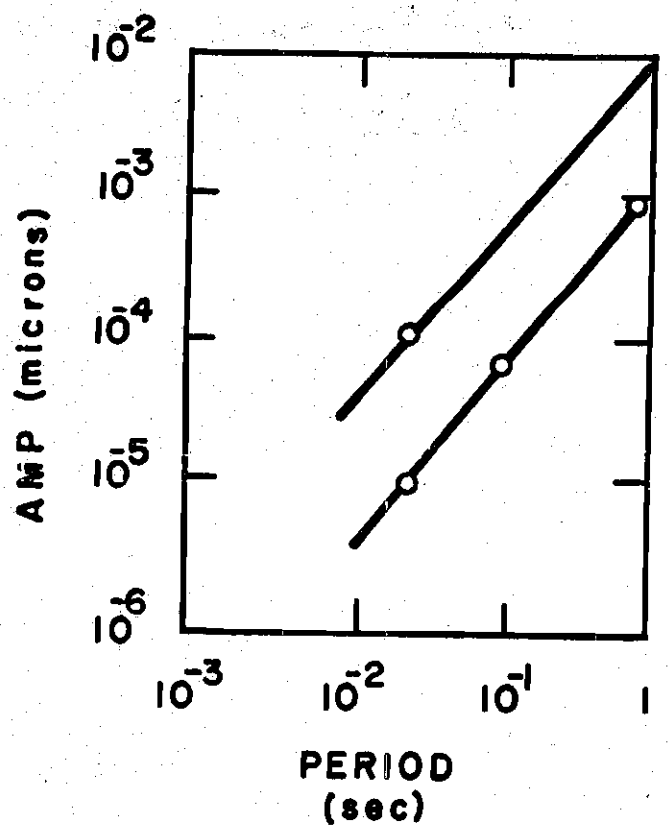

Figure 1. Surface Noise and Period from Brune (1959)

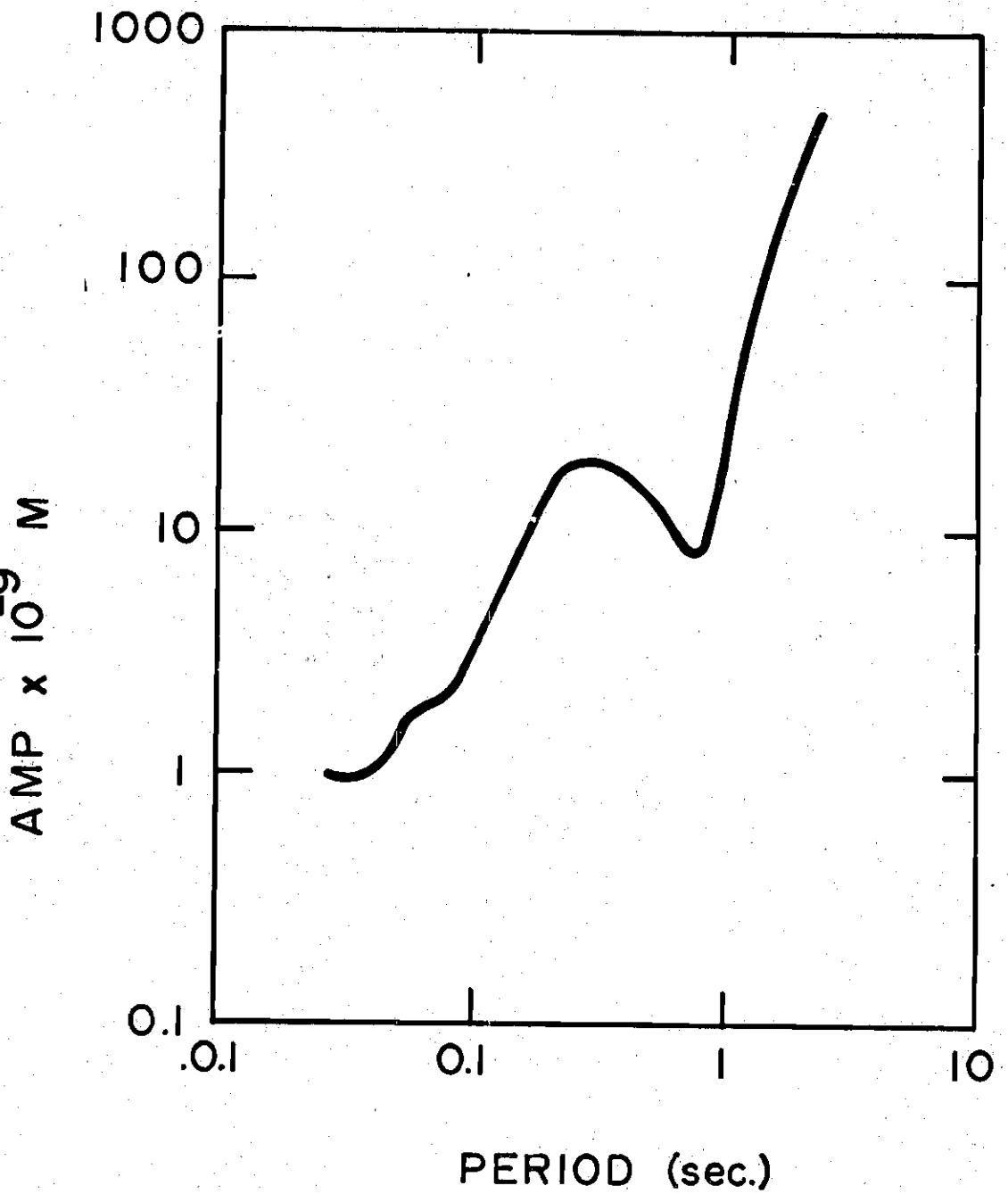

Figure 2. Noise Spectra in Ypsilanti, Mich. from Franti (1962)

studied by Long (1964). Seismic noise was propagated mainly as Rayleigh waves having spectral peaks at 2.9 and 3.4 Hz and a phase velocity between 1050 and 2200 ft./sec.

Douze (1967) postulated a theory wherein body and Rayleigh waves of modes higher than third order were responsible for the anomalous two Hz peak. He interpreted the noise with 0.3 to 0.8 second periods as being mostly of cultural origin.

Sanford, et al. (1968) studied train noise near Socorro, N.M. in that part of the spectrum below five Hz. He found the amplitude of seismic noise to be proportional to the length and speed of the train. Topography was also found to affect amplitudes of transmitted train seismic noise. From azimuths with large topographic relief train seismic noise was less intense than that from directions with less relief.

In an environmental impact study of seismic road noise, Long (1971) found the average seismic noise in the Atlanta, Georgia suburbs to have a particle velocity of 5.0×10^{-3} mm./sec., in the urban area 3.0×10^{-2} mm./sec., and in the rural area 1.8×10^{-3} mm/sec. In the 5 to 25 Hz frequency range one or more spectral peaks were found. The exact number and character depend on the location and its geology. Kanai, et al. (1954, 1957) and Akamatu (1961) found spectral peaks on "firm" ground at 3 to 10 Hz and on "soft" ground at 1.5 to 3.0 Hz. Long (1971) also found that the amplitude of seismic noise caused by a semi-trailer truck (12,000 to 72,000 lbs.) is twice the amplitude of steady car traffic (15 to 60 cars/min.) or four times that of a single car. Vehicle speed was not found to be a significant factor in seismic noise amplitude. Topographic attenuation was estimated to be one db for each foot of

relief above ten feet.

Long (1971) gave an empirical formula for attenuation of seismic road noise as a function of distance from a road. For observed amplitudes of seismic road noise from steady auto traffic (15 to 60 cars/min.) the decay with distance followed the equation:

$$\text{Log}_{10} A = 4.5 - 1.25 \text{ Log}_{10} r$$

where A was the amplitude in mm./sec. x 10^{-3}, and r was the distance in feet from the road bed. This equation was valid for r between 100 and 1,000 feet.

The purpose of this thesis is to investigate the frequency content of the coupled vehicle-road system as a source of seismic road noise and to investigate the frequency characteristics of the seismic road noise propagated away from the road. Data were taken at distances ranging between 50 and 250 feet from the source and in the frequency range between 2 and 50 Hz. These distances constitute the most important range for possible detrimental environmental impact. Hopefully the data and analysis presented in this thesis will improve the understanding of seismic road noise and its environmental impact.

CHAPTER II

INSTRUMENTATION

The instrumentation used to measure the particle velocity of the ground consisted of two 1.0 Hz geophones, two seismic amplifiers, and one 2-channel strip chart recorder (Figure 3). For all elements the frequency response between 2 and 60 Hz was flat to within a tolerance level of 10% (Figure 4).

The geophones, two Hall-Sears HS-10's having the same natural frequency of 1.0 Hz but differing coil impedances, were both operated at 70% damping. Thus, the 360-ohm geophone produced 0.835 v./cm./sec. above two Hz, while the 560,000-ohm geophone produced 13.4 v./cm./sec. in the same frequency range. Integrated-circuit operational amplifiers were used to amplify the geophone signal to voltages suitable for a Hewlett Packard 7402 A dual trace strip chart recorder. The recorder was operated at a response sensitivity of 50 mv./mm., or more, and at paper speeds ranging up to 125 mm./sec.

Strip chart records of seismic road noise were enlarged 15 times with the aid of a microfilm reader, traced on graph paper, and digitized. Digitizing was done by recording the time and amplitude of peaks and troughs, and interpolating the amplitude at predetermined equal-time intervals with a cosine interpolation (see Appendix I: Data Reduction).

Comparison of wave traces from two adjacent geophones located 50 feet from the road bed shows that the frequency responses of the two

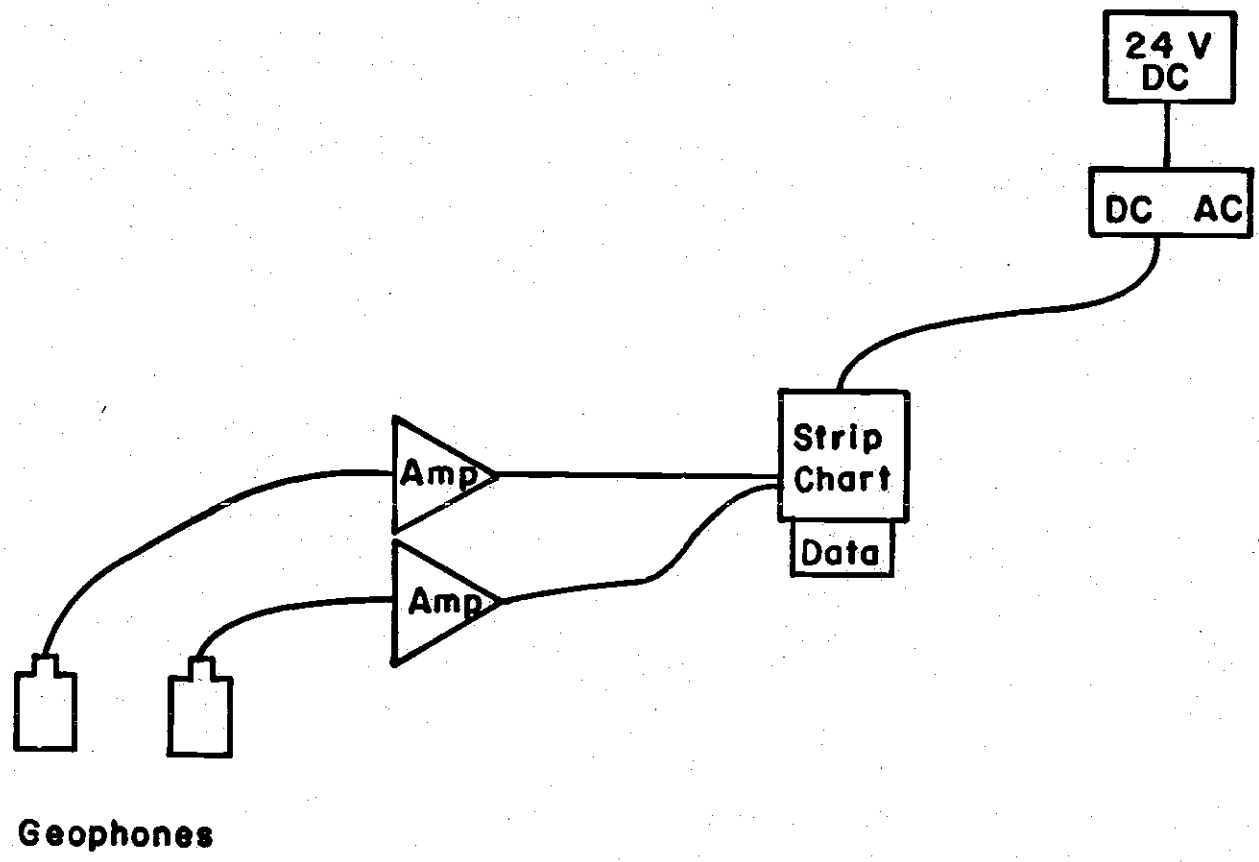

Figure 3. Instrumentation

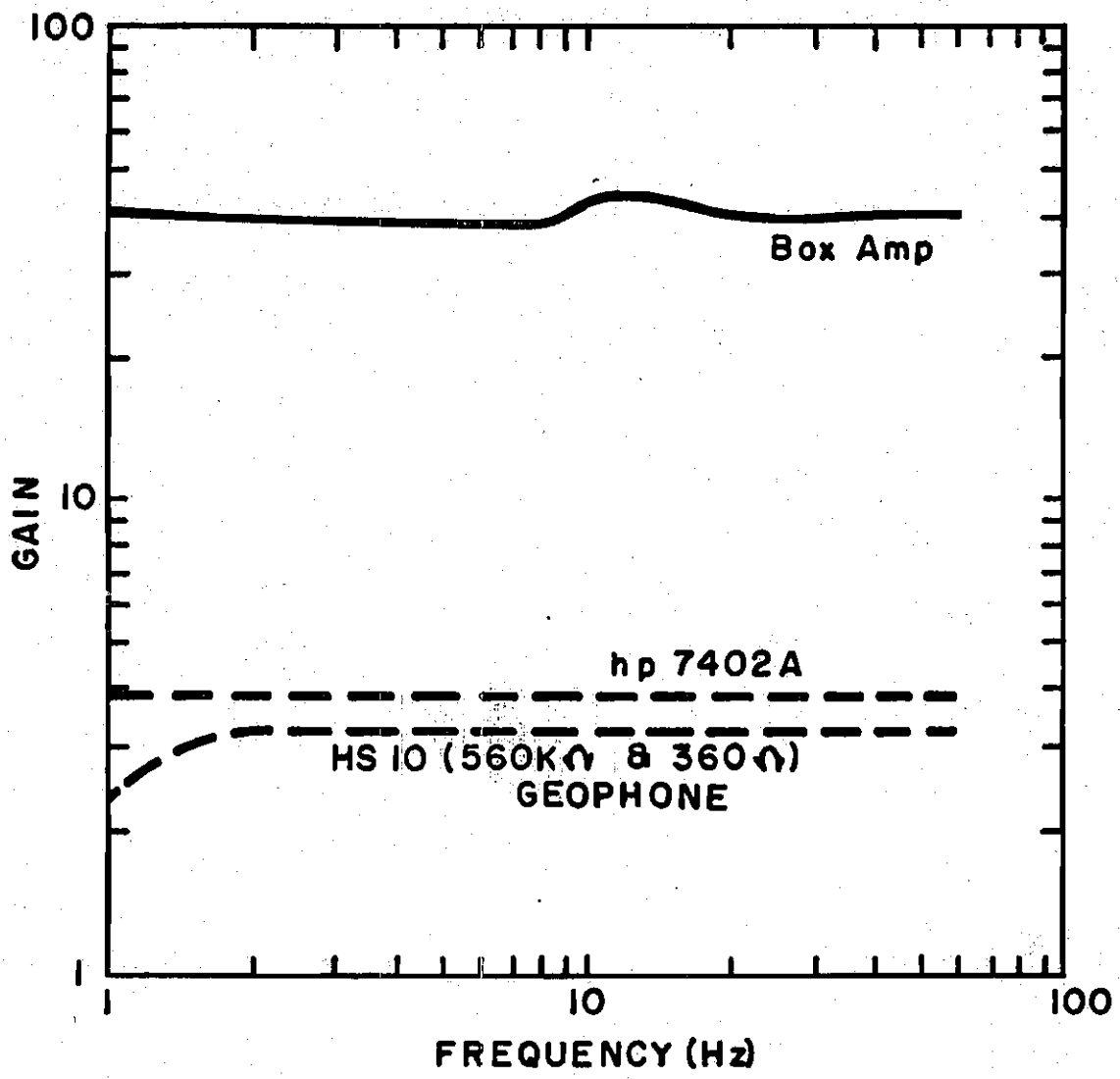

Figure 4. Frequency Response of Instruments

subsystems are virtually indistinguishable from each other (Figure 5). This comparison of instrument subsystems gives credibility to comparisons of particle velocities and uses of normalized spectra.

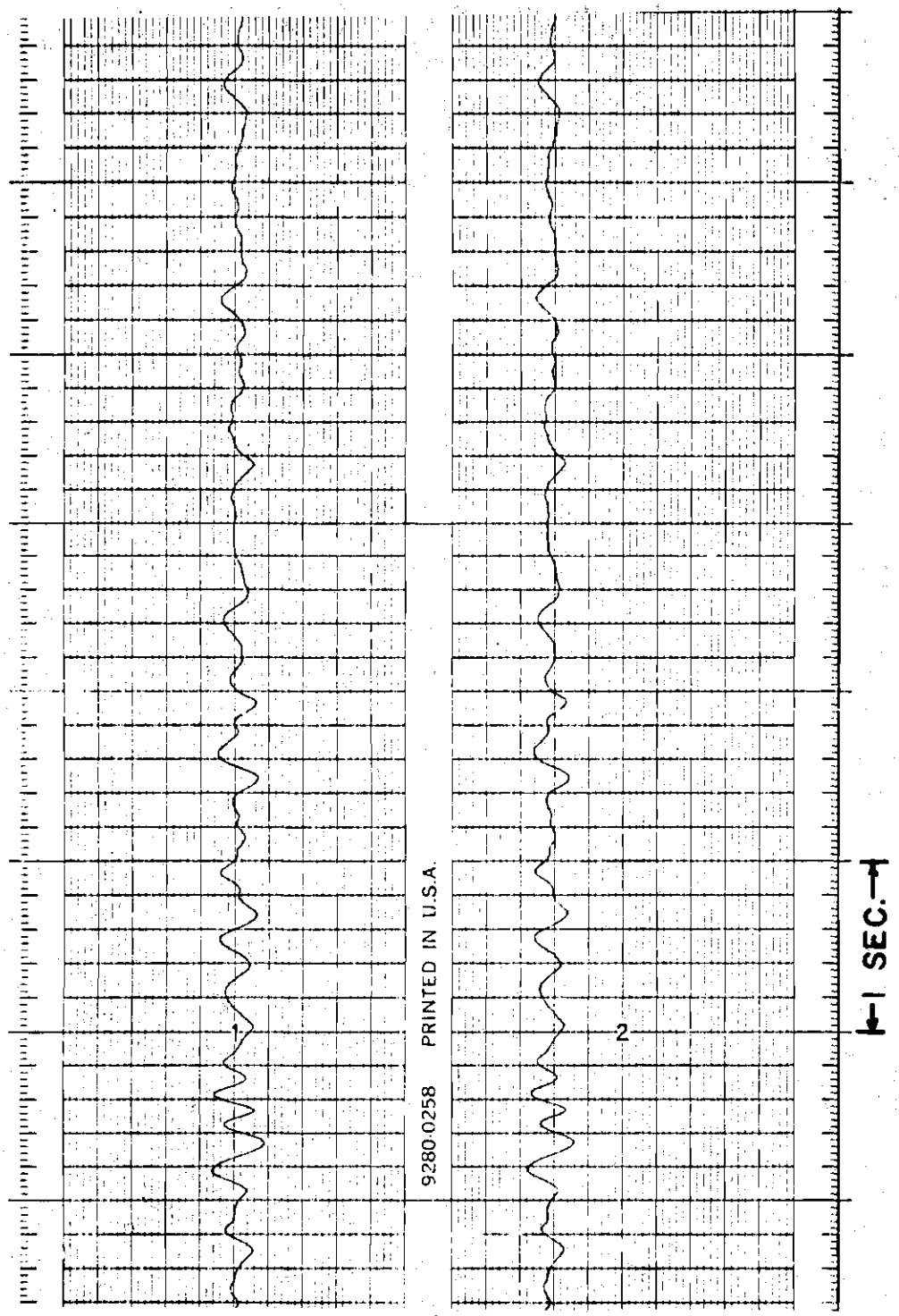

Figure 5. Response of Noise at Two Geophones At the Same Location

CHAPTER III

SOURCE OF SEISMIC ROAD NOISE

Data Collection

Observations of seismic road noise were initially made at 50 feet from the road bed measured from the middle of the near lane. At this distance the seismic road noise undoubtedly includes appreciable amounts of near field particle motion. Detectable levels of near field particle motions are usually confined to ranges of about a wavelength and are not propagated away from the source. For most seismic waves having frequencies below 6 Hz, wavelengths are significantly greater than 50 feet. The near field and far field seismic noise contributions decay, respectively, as $1/r^2$ and $1/r$, where r is the distance from a point source.

Vehicle size, vehicle speed, and particle velocity of the ground at a distance of 50 feet were recorded at five locations (see Appendix II: Locations). An average particle velocity was found by taking a one-second sample centered on the maximum particle velocity. In each chosen sample of magnified recorder trace the amplitudes of all positive peaks were measured and averaged. The measuring error was estimated to be ±5%.

Coupling

The source of seismic road noise is moving vehicles imparting motion into the ground through various coupling mechanisms. The source

can be thought of as a moving point source or as a moving finite block source (Figure 6). Some of the forward motion of the vehicle is converted into vertical motion by bumps, tire problems, and road depression. Bumps are the major source of seismic road noise. If a tire is unbalanced or has flaws in its roundness, vehicles move up and down transmitting momentum and therefore energy into the ground, comprising a second, although minor, source of seismic road noise. A fair estimation of the particle velocity a vehicle puts into the ground can be made by simply noting how the vehicle rides. In fact, a vehicle could be thought of as a complex inverse geophone in which the spring and damping system of the vehicle serve as a modifying factor in transforming vertical forces of the moving vehicle into corresponding ground motions. The way the vehicle moves up and down, determines the character of the particle velocity. Road depression is the displacement caused by the moving vehicle's weight on the road. Figure 6 shows one example of a vehicle on a sectioned road causing road depression.

On interstate highways, seams, and even dirt, cause vehicles to bounce. On lower quality roads where the size and frequency of occurrence of bumps increase the seismic road noise increases accordingly. Mather (1963) found that dirt roads become corrugated, because a wheel pushes dirt in front of itself until enough dirt collects to form a bump. The distance between bumps is dependent on the wheel's speed and the type of dirt.

The nature of the rock underlying the road bed affects both the generation of seismic road noise and the way it is transmitted to the geophones. The amount of elastic coupling between the road and underlying

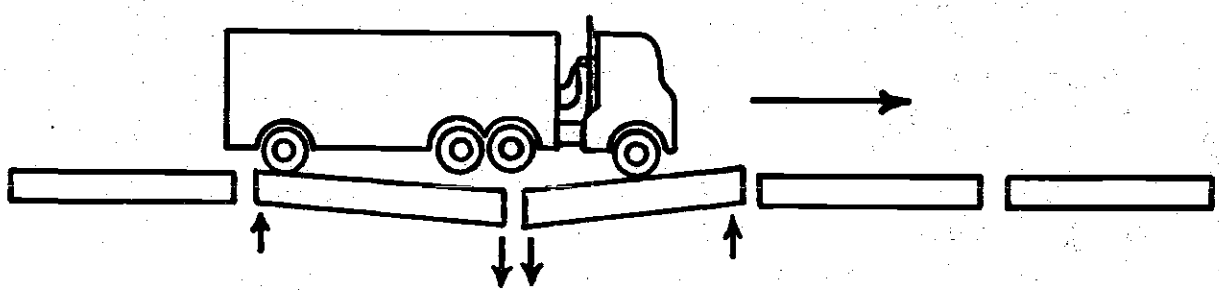

Figure 6. Road Depression

rock determines how much the ground moves. The elastic wave conducting characteristics of the underlying rock then also determines the amplitude decay with distance. Therefore, road type and underlying rock both effect seismic road noise.

Seismic road noise in Coastal Plain sediments at locations (Figure 7; SR5 and SR6) have smaller particle velocities than seismic road noise measured at the same distance on Piedmont Province rocks (Figure 7; SR4). Particularly noteworthy were the particle velocities associated with the massive granite outcrop at location SR2 as compared with measurements on Coastal Plain sediments.

Locations SR5 and SR6 had different seismic noise levels due to the road type (two lane and interstate, respectively). Both these stations were on Coastal Plain sediments. Medium-size cars (~3500 lbs.) operating in the speed range between 45 and 65 mph created twice as much seismic noise on the two lane road as they did on the interstate highway.

Effects of a Vehicle's Speed and Weight

The speeds of vehicles were determined by measuring the time they took to travel 90 feet. The use of traffic as a source has inherent problems, especially in relation to individualizing the source and timing the vehicle over the measured course. However, based on errors of ±2 feet in the distance and ±0.08 seconds in the time, it was possible to determine a vehicle's speed to an accuracy of ±3 mph.

Particle velocities of the ground corresponding to the passage of vehicles were plotted against vehicle speeds at five separate locations (Figure 7). At locations SR5 and SR6 semi-trailer trucks (12,000 to

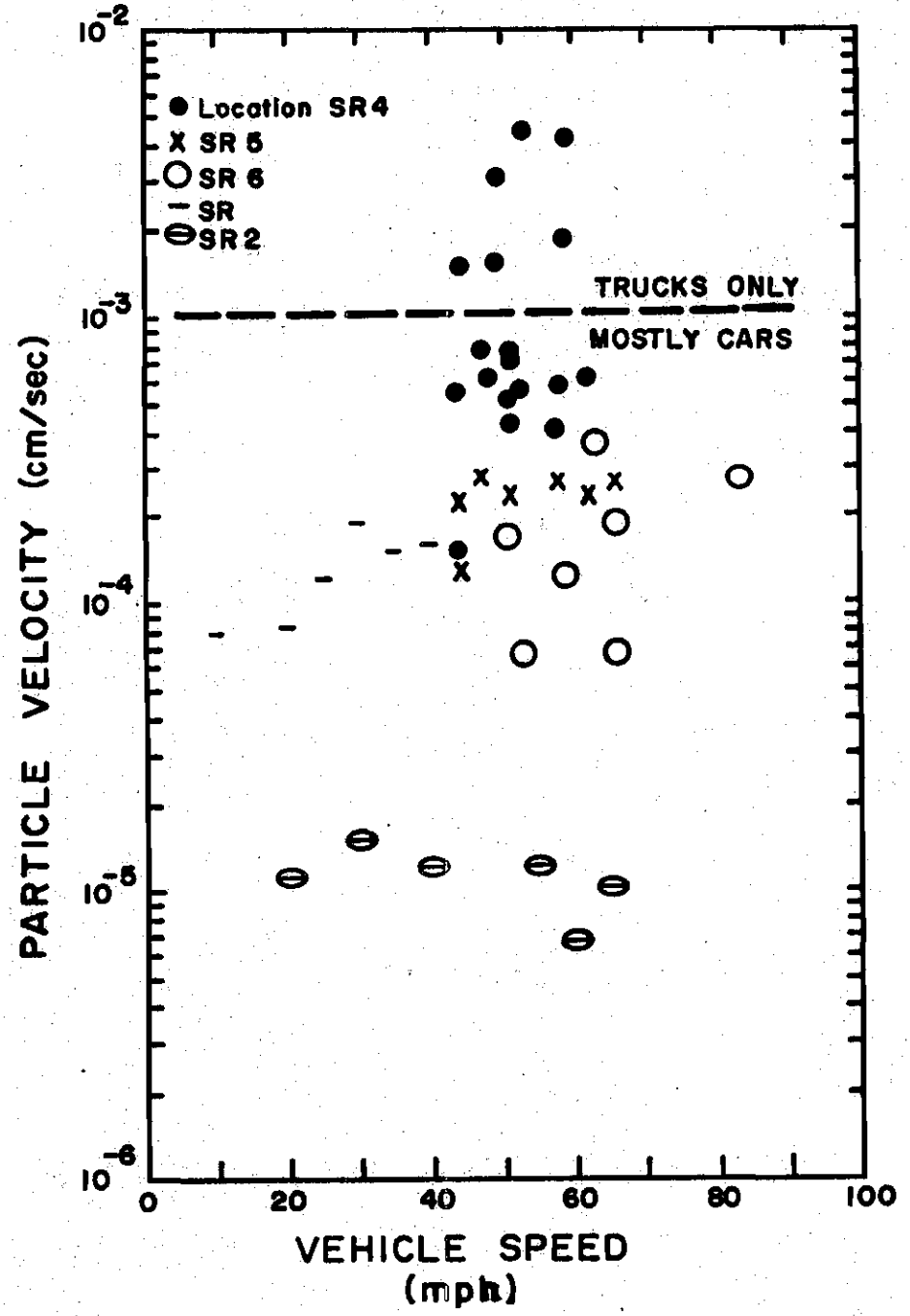

Figure 7. Particle Velocities of Vehicle Speeds at Various Locations

72,000 lbs.) had particle velocities two to four times that of a single car (~3500 lbs.), consistent with Long's (1971) results.

Shown in Table 1 are the particle velocities of four cars going 51 mph at location SR4. In this case the vehicle's weight was not an important factor effecting seismic noise levels. Note: the Vega had the largest particle velocity. From all data (see Appendix III: Source), semi-trailer trucks usually had the largest particle velocities.

Table 1. Car Type, Car Weight, and Particle Velocity at Location SR4 of Vehicles Going 51 mph.

Car Type	Approximate Weight (lbs.)	Particle Velocity (cm./sec.)
Pontiac	4200	5.36×10^{-4}
Vega	2500	7.56×10^{-4}
VW	2000	4.41×10^{-4}
Pick-up	3500	7.25×10^{-4}

CHAPTER IV

SEISMIC ROAD NOISE PROPAGATION

Data Collection

The change in frequency content of a wave as it travels across the ground from the road bed to the geophone can be examined by Fourier analysis (see Appendix I: Data Reduction). The spectral modulus is proportional to the amount of energy in a distinct frequency interval.

Data for the Fourier analysis were waves from the strip chart recorder digitized for one-second samples. The one-second samples were centered on the maximum amplitudes. The measuring error for digitizing data was 0.5% for time and 5% for amplitude. Consequently, when measuring amplitudes below one-tenth maximum spectral modulus, the data were meaningless, because on the average about 50% of the trace amplitude was noise. At frequencies above 40 Hz moduli were often below this level. Using a digitizing increment of 0.01 second, the folding frequency is 50 Hz and therefore within the flat frequency response range of all instruments. An example of spectra is shown in Figure 8.

The spectra of ground motion at a distance of 50 feet were different for different passes of the same car traveling at the same speed over the same portion of road. Presumably, this difference was due to the car going over different bumps in the road in each pass. Figure 9 shows sepctra at 50 feet for locations AT and AT4. To study the

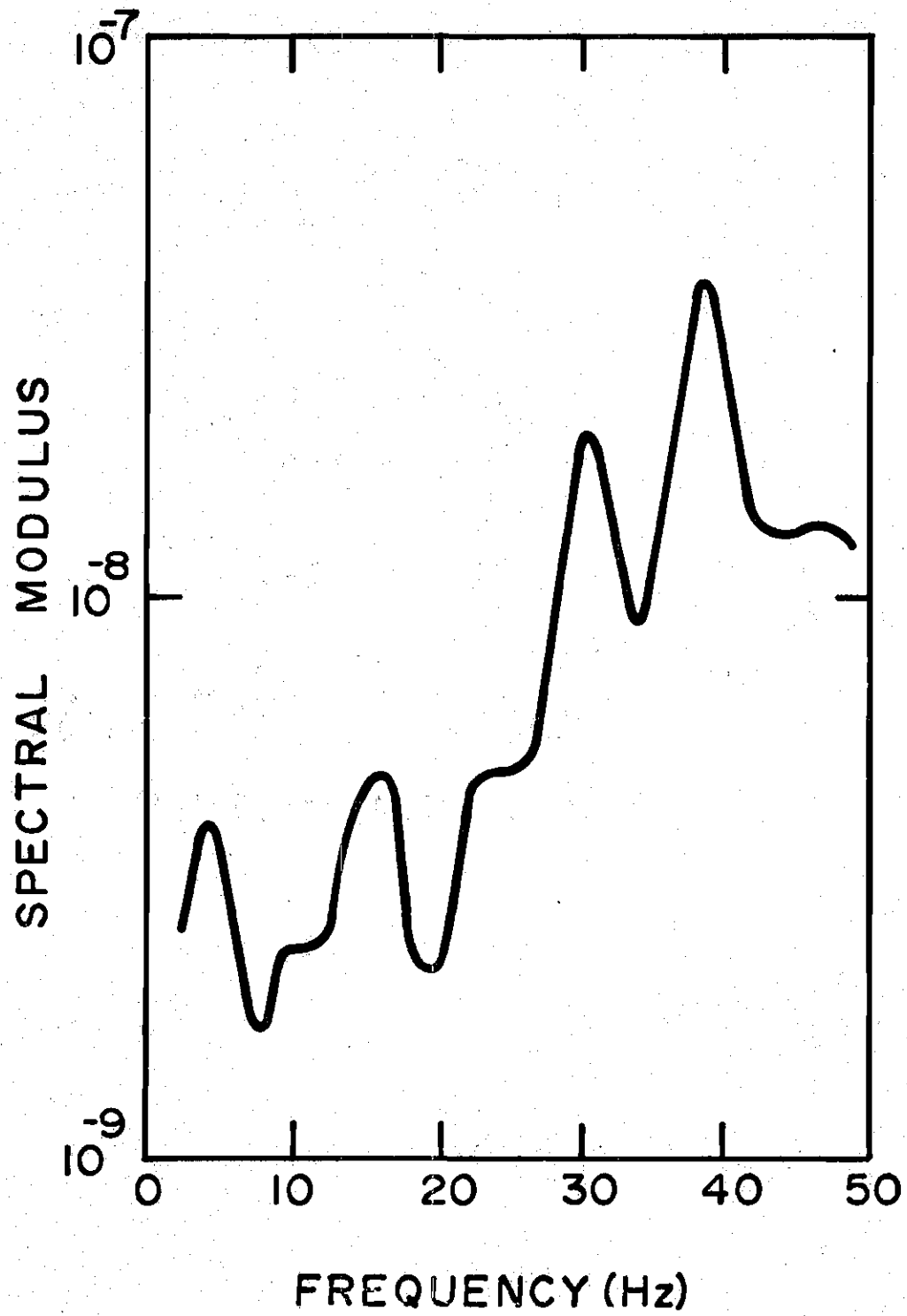

Figure 8. Spectra of Seismic Road Noise

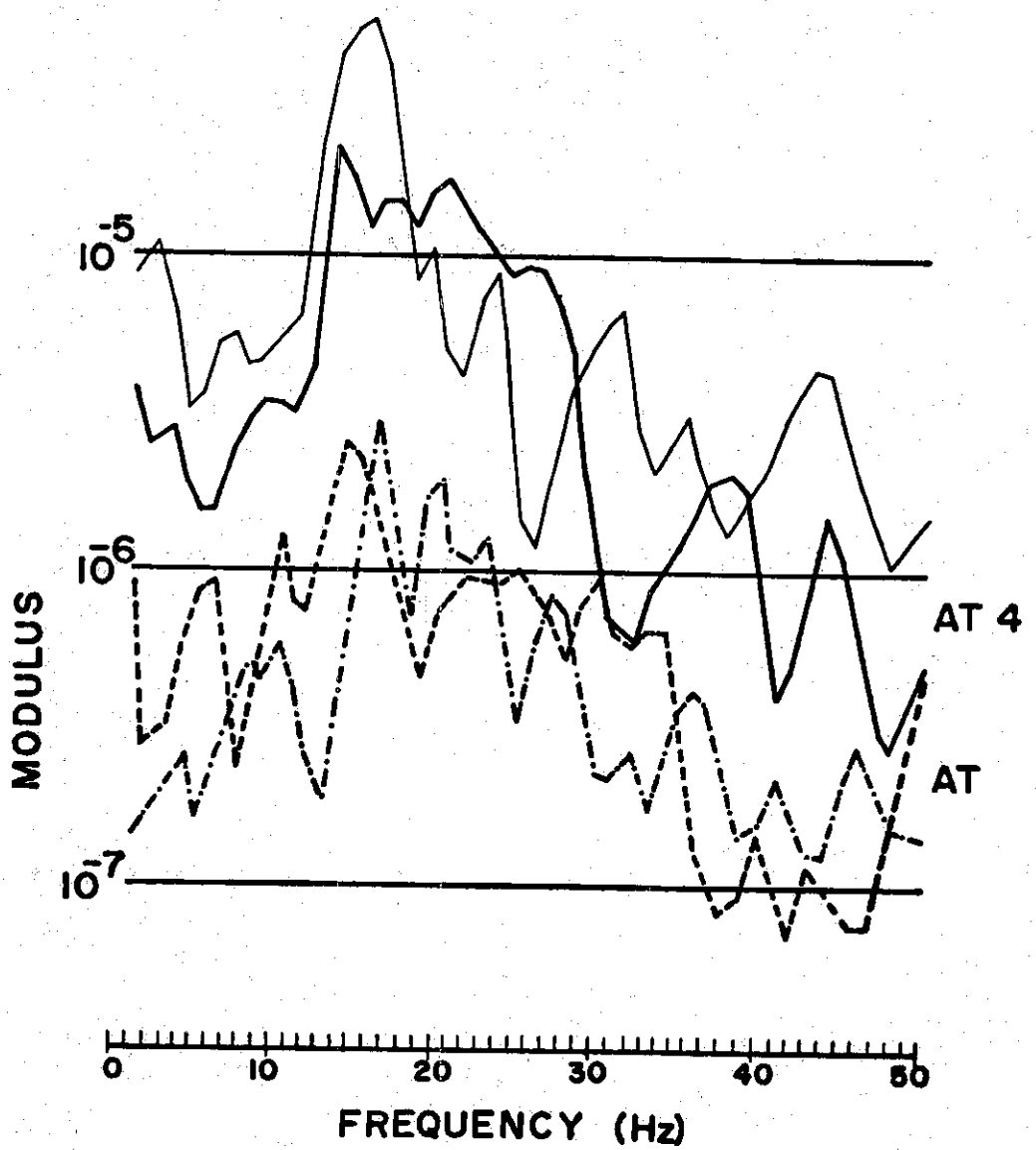

Figure 9. Spectra at 50 Feet from Locations AT and AT4

change in spectra with distance, spectra taken at variable ranges between 50 and 250 feet were normalized to the standard spectrum taken simultaneously at 50 (or 100) feet. The experiment was always arranged so that energy propagating over the path always had an isolated section of a single road as the signal source (Figure 10). The geophone assembly in Figure 3 was used with one geophone at 50 (or 100) feet as a standard.

Spectral Changes with Distance

Figure 11 shows seismic noise spectra as a function of distance from the road bed for locations AT and AT4. Normalized to 50 feet, location AT had three spectral peaks at 38, 42, and 45 Hz at a distance of 100 feet and one major peak at 13 Hz at 150 feet. At 100 feet, there was also a low at 9 Hz for the normalized spectra. At 150 feet location AT4 had three normalized spectral peaks at 31, 42, and 47 Hz. At 250 feet one normalized spectral peak was noted at 7 Hz. As distance from the road increased a decrease in frequency of the average maximum normalized modulus was observed (Figure 12).

Spectra normalized to 50 feet often showed a tendency to behave in an unpredictable fashion. In an attempt to reduce this variation, the standard geophone was placed at 100 feet and the spectra normalized to that distance. The 50 foot spectra normalized to 100 feet approach white noise, with five to eight roughly equal peaks between 2 and 40 Hz (Figures 13, 14, and 15). At 50 feet, the normalized spectra moduli for medium-sized cars (Figure 14) are smaller between 25 and 40 Hz than those for semi-trailer trucks (Figure 15). At a 250 foot

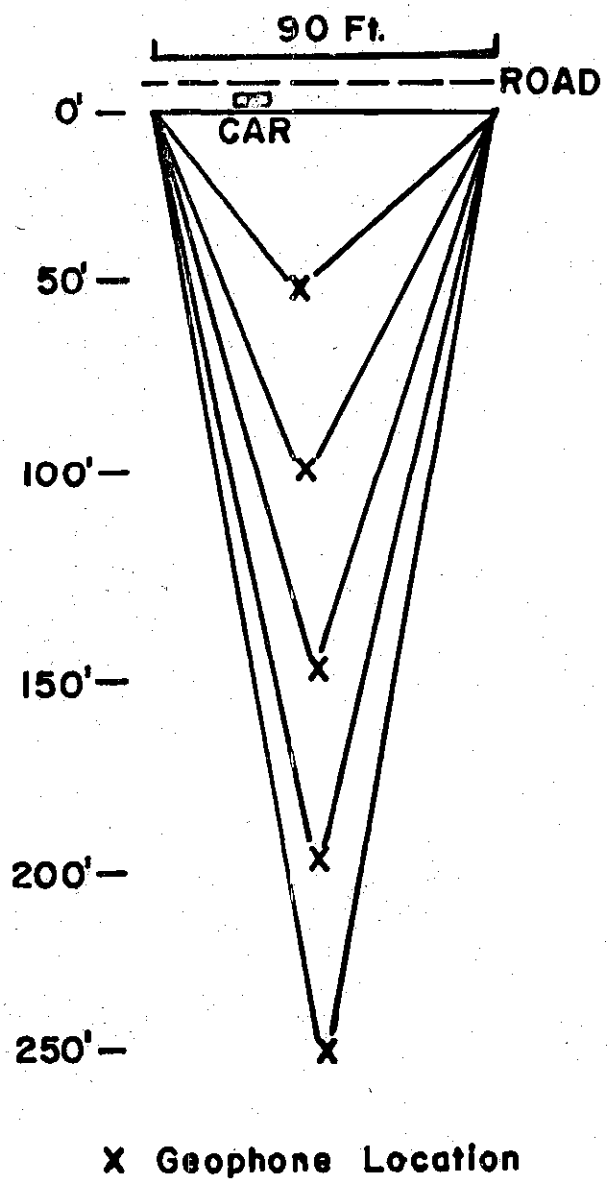

Figure 10. Paths of Wave Propagation for Different Geophone Locations

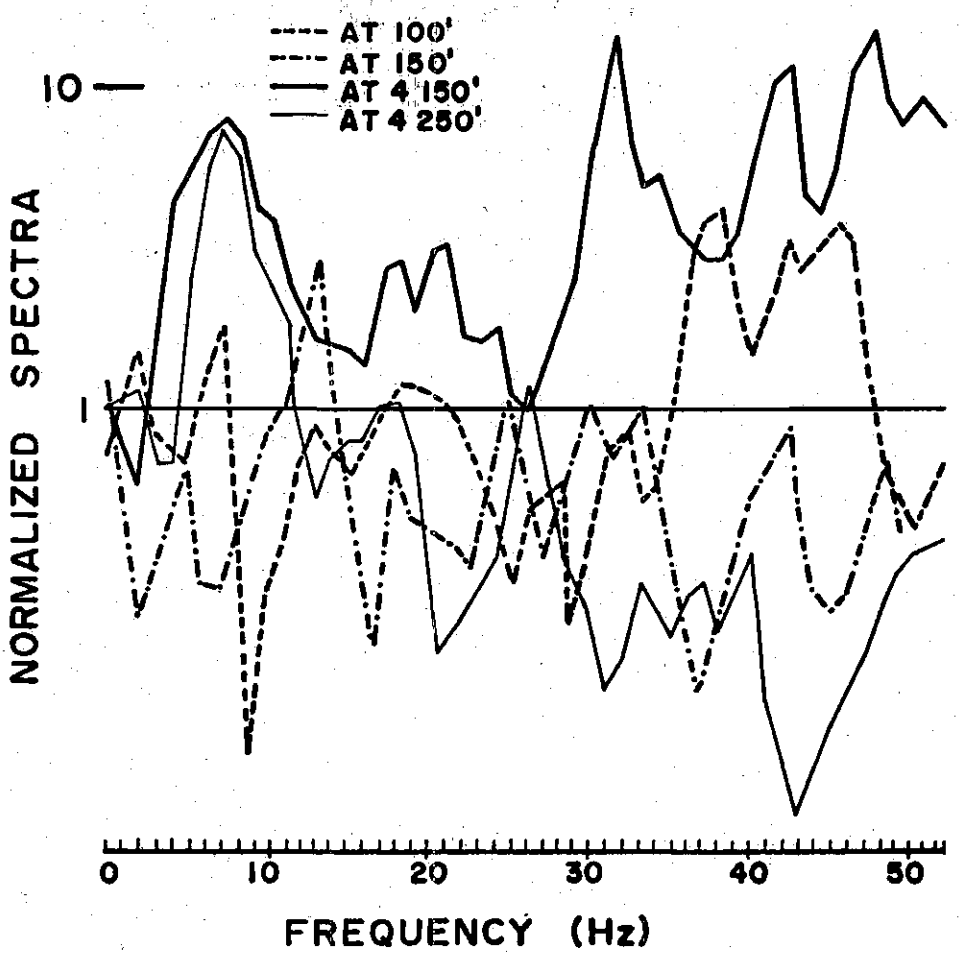

Figure 11. Normalized Spectra with Distance at Locations AT and AT4

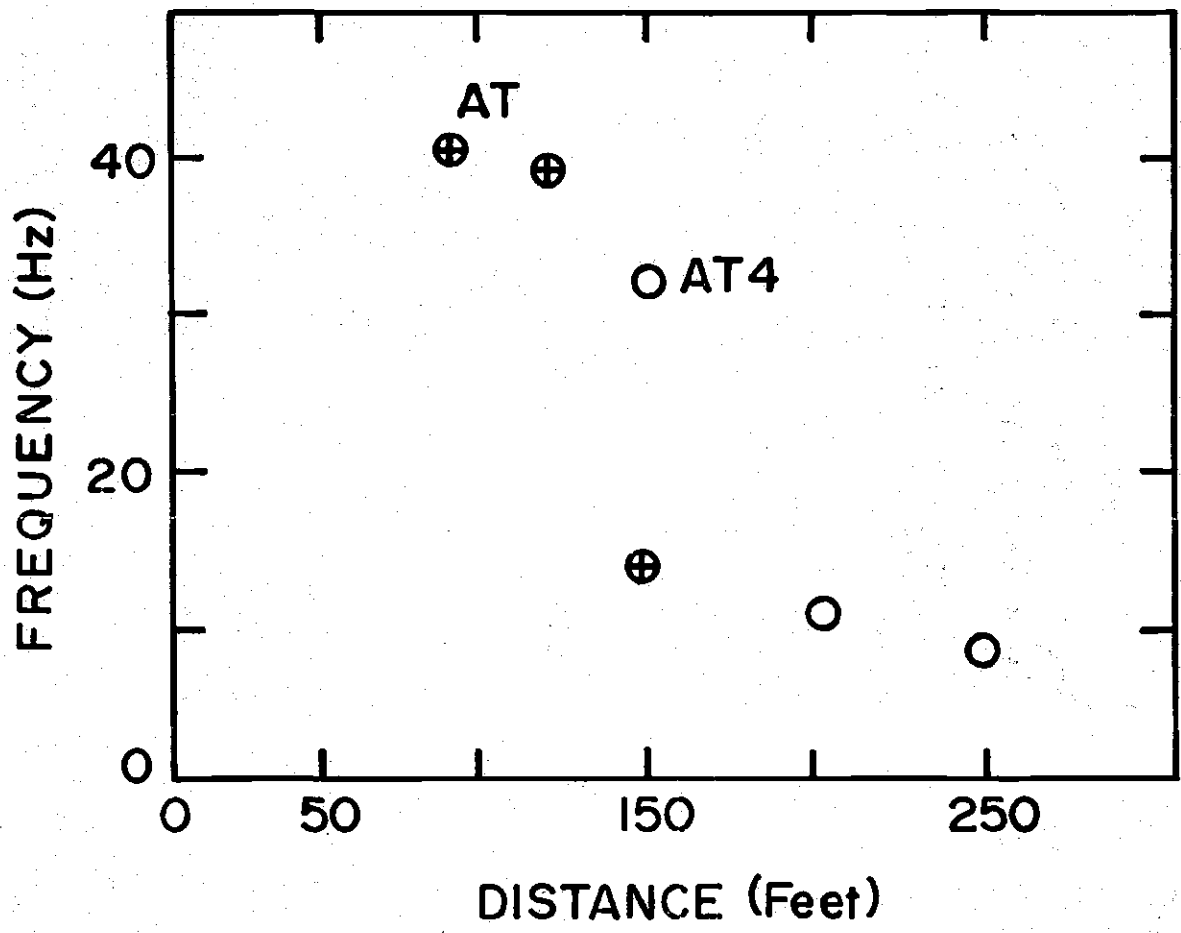

Figure 12. Frequency of Average Maximum Normalized Modulus and Distance from Road Bed

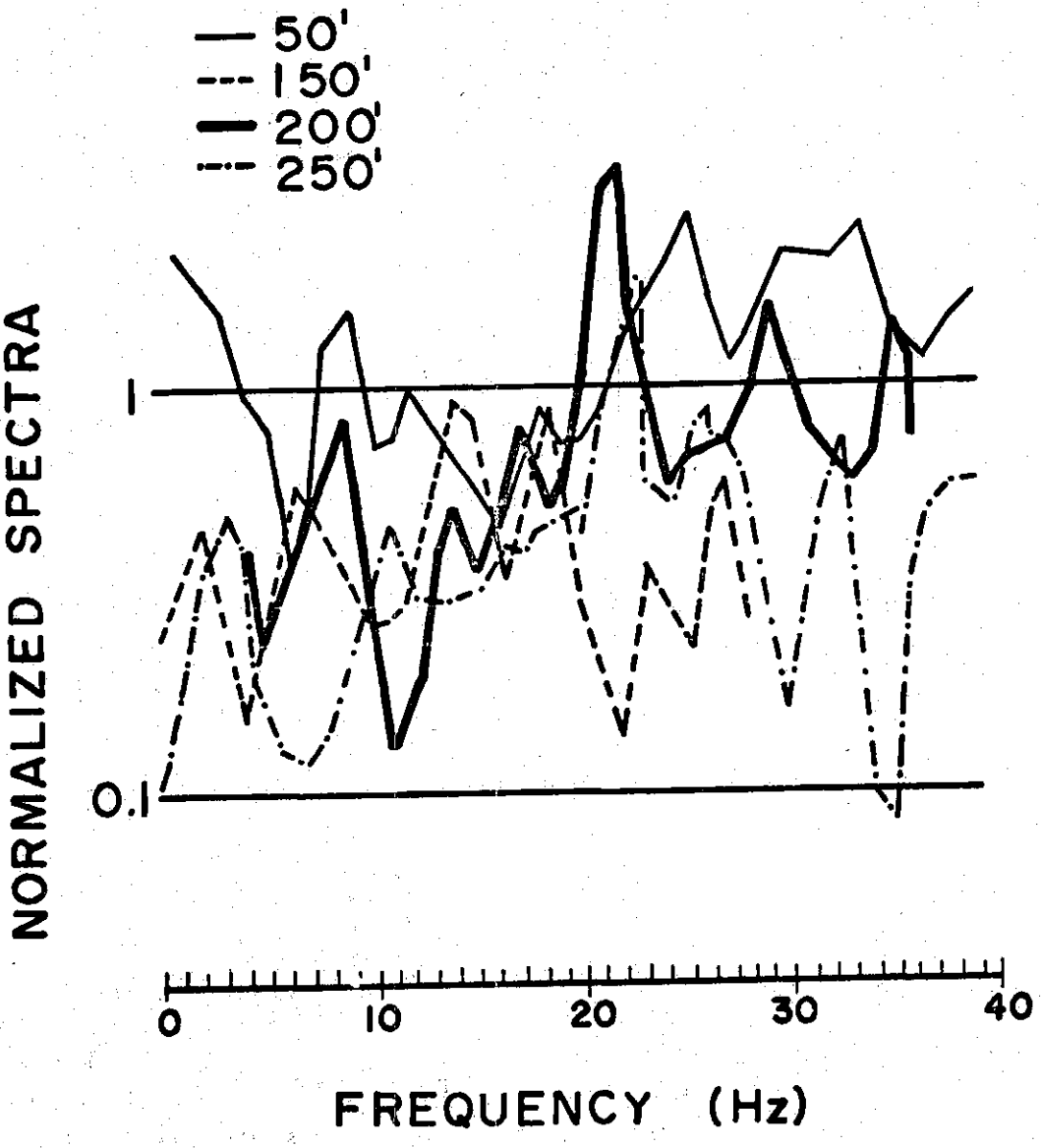

Figure 13. Normalized Spectra at Various Distances at Location AT10

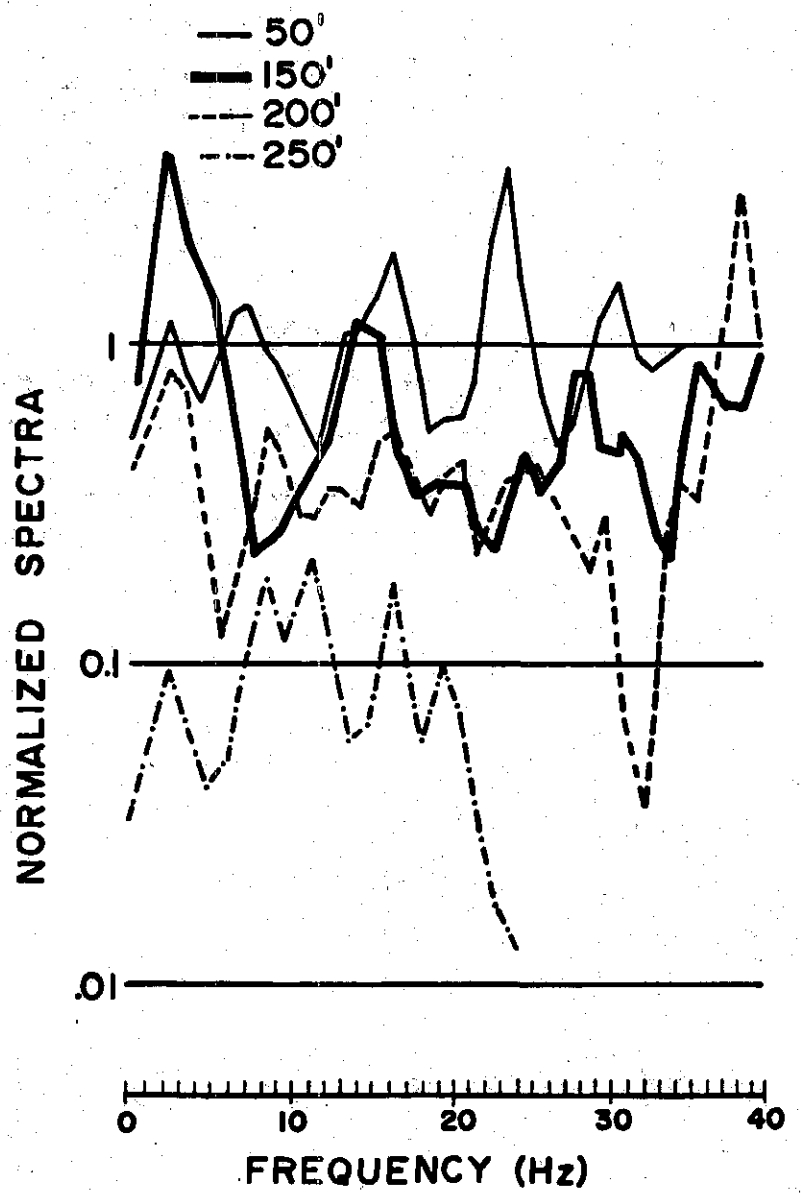

Figure 14. Normalized Spectra of Cars at Various Distances at Location AT11

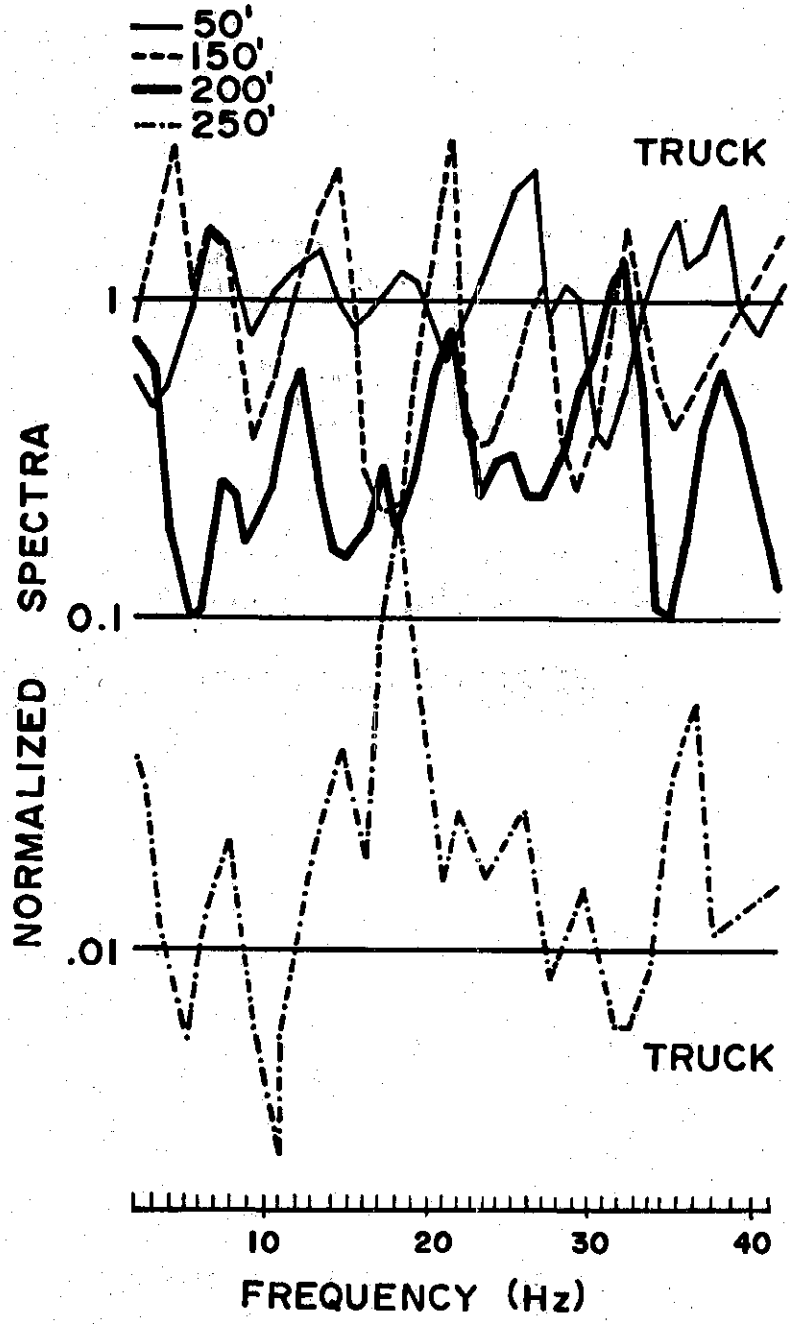

Figure 15. Normalized Spectra for Semi-Trailer Trucks at Various Distances at Location AT11.

distance at location AT11, the large input of energy from semi-trailer trucks showed a single large spectral peak at 18 Hz in the spectrum normalized to 100 feet (Figure 15), while medium-sized cars at that range and location gave four peaks at 9, 12, 17, and 20 Hz.

Figure 16 compares the data from Figure 13, 14, and 15, showing the variation of the normalized moduli with frequency and distance from the road bed; these data are also compared with Long's (1971) empirical relation between amplitude and distance from the road (an amplitude normalized to the amplitude at 100 feet was used).

Spectral Changes with Rock Type

To study the effects of rock type on spectrum character, spectra from AT4, a location underlain by hard rock, were compared with those from AT, where clay fill predominated (Figure 9 and 11). For location AT4 at 150 feet a large amount of high-frequency (28 to 50 Hz) seismic noise was apparent (Figure 11). The most significant change in spectrum character is an amplification of the seven Hz normalized spectral peak. At 150 feet the hard rock was a more efficient carrier of high-frequency (28 to 50 Hz) energy than soft rock as can be seen by the presence of the three normalized spectral peaks at 31, 42, and 47 Hz. At 50 feet the soft rock spectral modulus was about one-tenth as large as the hard rock spectral modulus (Figure 9). This change in energy carrying characteristics between hard rock and soft rock is also seen in Figure 12. At 150 feet the average maximum normalized modulus for hard rock was at a frequency of 34 Hz while for soft rock it was at 18 Hz.

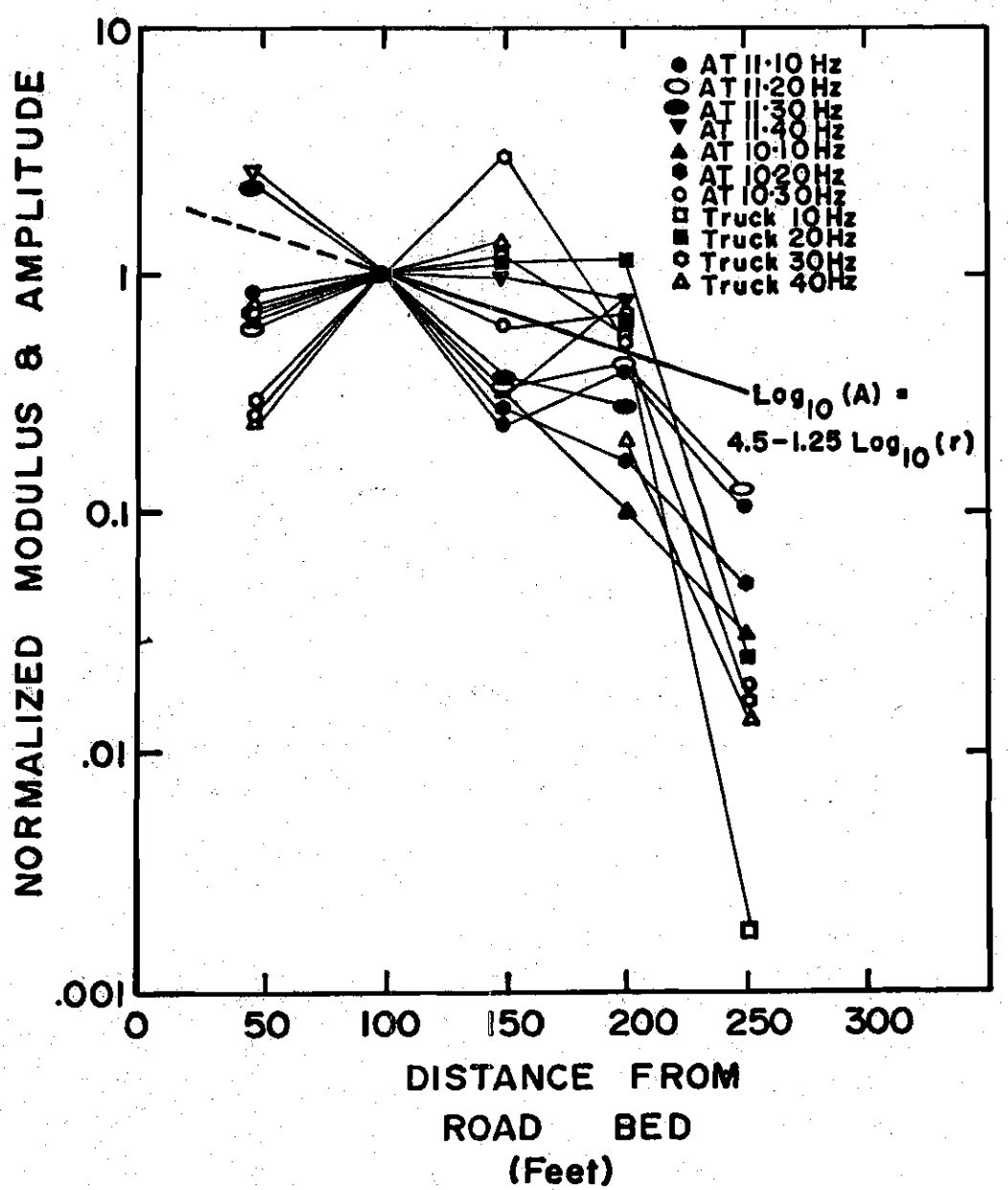

Figure 16. Comparison of Normalized Modulus and Distance from Road Bed

CHAPTER V

DISCUSSIONS & CONCLUSIONS

The character of seismic road noise, which has been defined as ground vibration derived from vehicle motion, was found to be dependent on the weight of the vehicle and the geologic setting of the road bed. The type of springs on the vehicles and spacings of bumps in the road also seemed to be major factors in how the vehicle transmitted energy into the ground. Measuring particle velocities at 50 feet in order to establish a standard spectrum for comparison and simultaneously at 100, 150, 200, and 250 feet to observe spectral changes with distance revealed no simple explanation for the earth's filtering system.

The particle velocities at five locations for vehicles at a distance of 50 feet from the road bed are shown in Figure 7. Of these, location SR4, a clay fill, had the largest particle velocities. Here, medium-sized cars (~3500 lbs.) produced particle velocities twice as large as those caused by similar cars at the next most similar location, SR5, on the Coastal Plain; three to four times the particle velocities at locations SR and SR6, both on "soft rock", (the first on the Piedmont and the second on the Coastal Plain); and 50 times that at location SR2, a massive granite outcrop. These variations seem consistent with road type and geologic location.

Generally, hard rock is a more efficient propagation of seismic energy than alluvium, or even soft rock. Also, hard rock has a greater elastic modulus. Thus, a given stress results in greater strain in

alluvium or soft rock than in hard rock, so that a moving vehicle deforms the road surface more if the later is underlain by soft rock rather than hard rock. Futhermore, since particle velocity is proportional to the first time-derivative of the particle displacement, for frequencies above 1 Hz the particle velocities are further exaggerated in the less resistant materials. This accounts not only for hard rock having a smaller particle velocity than soft rock at 50 feet but also for hard rock being a more efficient carrier of high-frequency (28 to 50 Hz) energy. Figure 9 illustrates this filtering and attenuation of energy by the earth.

At a distance of 250 feet the dominant normalized spectral peak (Figure 15) is 18 Hz. This is probably the residual remaining after the higher frequency components of the signal put in by the semi-trailer trucks (predominantly 28 to 50 Hz) were attenuated. The average maximum normalized modulus (Figure 12) occurs at lower frequencies as the distance from the road bed increases.

The range of distances from 50 to 250 feet constitute the most important distances in which seismic road noise could possibly have environmental impact. These data along with considerations about types of traffic on particular roads, natural frequencies of building motions, and types of road beds may help reduce the environmental impact of seismic road noise.

CHAPTER VI

SUGGESTIONS FOR FURTHER INVESTIGATION

1) Data should be taken from a larger variety of geologic conditions. There may be a correlation between rock type and normalized spectral peaks.
2) By using a smaller digitizing increment, higher frequencies could be studied.
3) The use of horizontal component geophones would help clarify the wave types which contribute to seismic road noise.

APPENDIX I

DATA REDUCTION

The program which follows takes the peaks and troughs of wave forms (corrected to sec. and cm./sec.) and uses a cosine interpolation (subroutine Digi) to obtain digital data. These data are run through subroutine sertra (a Fourier transform). A Fourier transform changes a series in the time domain, $Z(t_i)$, i = 1, N, into the frequency domain, $Z(f_j)$, j = 1, N. The transform pair is as follows:

$$Z(t_i) = \sum_{j=1}^{N} Z(f_j)\, e^{i2\pi f_j t_i}\, dt$$

and

$$Z(f_j) = \sum_{i=1}^{N} Z(t_i)\, e^{-i2 f_j t_i}\, df$$

where $Z(f_j)$ is a complex amplitude and is a discrete function of f, the frequency. Because $Z(f_j)$ is complex it takes the form:

$$Z(f_j) = R(f_j) + i\, I(f_j)$$

where $R(f_j)$ is the real or even component and $I(f_j)$ is the imaginary or odd component of the transform. This gives a modulus:

$$[Z(f_j)] = (R(f_j)^2 + I(f_j)^2)^{1/2}$$

```
1*            DIMENSION H(1000),T(1000),A(1000),LABEL(500),AFREQ(500),PH(500),
2*           *BFREQ(500),SFREQ(500),F(500)
3*      C THIS PROGRAM COMPUTES SPECTRA FOR DATA INPUTTED AS
4*      C NODES. CORRECTION FACTORS ARE NEEDED FOR AMPLITUDEA (HC)
5*      C AND TIME (TC) TO GET THE UNITS CM/S, AND S.
6*      C FORMATTED INPUTS ARE NEEDED FOR INITIAL TIME (TI), NO.OF
7*      C POINTS OF DIGITIZED DATA WANTED (NDT), TIME INVERAL
8*      C (DT), NO. OF NODES INPUT (NI)
9*            1 READ(5,4)(LABEL(I),I=1,13)
10*           4 FORMAT(13A5)
11*             READ (5,3) TI,NDT,DT,NI,HC,TC
12*           3 FORMAT (1F5.3,1I3,1F5.3,1I4,2E10.2)
13*             READ (5,2,END=999)(T(I),H(I),I=1,NI)
14*           2 FORMAT (5(1F5.0,1F5.1))
15*             DO 54 I=1,NI
16*             T(I)=T(I)*TC
17*             H(I)=H(I)*HC
18*          54 CONTINUE
19*             WRITE(6,5)(LABEL(I),I=1,13)
20*           5 FORMAT(10X,30X,13A5///)
21*             WRITE(6,9)(T(I),H(I),I=1,NI)
22*           9 FORMAT (6E10.4)
23*             CALL DIGI(H,T,N,TI,NDT,DT,F)
24*             N=NDT
25*             DO 46 I=1,N
26*             A(I)=F(I)
27*          46 CONTINUE
28*             WRITE(6,6)N,DT
29*           6 FORMAT(40X,'NUMBER OF DIGITIZED POINTS = ',I5,'   TIME INTERVAL =',
30*            1,F10.8,' SEC'//)
31*             WRITE(6,7)
32*           7 FORMAT(50X,'DIGITIZED DATA'//)
```

```
33*           WRITE(6,9)(A(I),I=1,N)
34*           WRITE (6,21)
35*        21 FORMAT(1H1/,9X,'PLOT OF AMPLITUDE VERSUS TIME'//)
36*           WRITE(6,5)(LABEL(I),I=1,13)
37*           CALL MXSCL(N,A,AMAX)
38*           CALL DRAW(N,1,A,AMAX)
39*           DF=1.0/(N*DT)
40*           NW=100./DF+1
41*           WRITE(6,19)
42*        19 FORMAT(1H1//,30X,'RAW SPECTRAL DATA (NOT CORRECTED FOR INSTRUMENT
43*          *RESPONSE OR SMOOTHED)')
44*       112 FORMAT(//17H DIRECT TRANSFORM,6H WO = ,2E17.7/10H   MODULUS,
45*          110H AND PHASE/ (1X,E15.6,F10.2,E15.6,F10.2,E15.6,F10.2,E15.6,F10.2
46*          2,E15.6,F10.2))
47*           CALL SERTRA(0.0,N,NW,DF,AFREQ,PH,WO,A)
48*           NW=NW-1
49*           WRITE(6,11)
50*        11 FORMAT(1H1 ,9X,'PLOT OF LOG10 SPECTRA VERSUS FREQUENCY'//)
51*           WRITE(6,5)(LABEL(I),I=1,13)
52*           DO 17 I=1,NW
53*        17 BFREQ(I)=AFREQ(I)
54*           CALL MXSCL (NW,BFREQ,AFMX)
55*           CALL DRAWML(NW,1,BFREQ,4.,AFMX,DF)
56*           SFREQ(1)=AFREQ(1)
57*           SFREQ(NW)=AFREQ(NW)
58*           NL=NW-1
59*           DO 14 I=2,NL
60*           K=I+1
61*           L=I-1
62*           SFREQ(I)=(AFREQ(I)+AFREQ(L)*.5+AFREQ(K)*.5)/2.
63*           IF(SFMX.GT.SFREQ(I))GOTO 14
64*           SFMX=SFREQ(I)
```

```
1*            SUBROUTINE SERTRA(DET,N,NW,DF,G,PH,WO,T)
2*      C    DET = 0 TIME TO FREQ DOMAIN, NOT = 0 FREQ TO TIME, N=NUMBER OF TIME POINTS
3*      C    NW=N/2 OR NO. OF FREQUENCY PTS. OF = FREQ INTERVAL = 1/T, T=N*DT
4*            DIMENSION G(NW),PH(NW),T(N),CFN(500),SFN(500)
5*            PI = 3.1415926536
6*            CF = 0.0174532925
7*            AN = N
8*            DO 119 I = 1,N
9*            A = I
10*           ARG = (6.28318531*A)/AN
11*     119   CFN(I) = COS(ARG)
12*           SFN(I) = SIN(ARG)
13*           IF (DET) 131,132,131
14*     132   DO 133 I = 1,NW
15*           G(I) = 0.0
16*     133   PH(I) = 0.0
17*           WO = 0.0
18*           DO 139 J = 1,NW
19*           X = 0.0
20*           Y = 0.0
21*           DO 140 I = 1,N
22*           IJ = I*J - N*((I*J-1)/N)
23*           X = X + T(I)*CFN(IJ)
24*     140   Y = Y - T(I)*SFN(IJ)
25*           PH(J)=(ATAN2(-Y,-X))/CF +180.
26*     139   G(J) = (1.0/(AN*DF*6.28318531))*SQRT(X*X + Y*Y)
27*           DO 134 I = 1,N
28*     134   WO = WO +T(I)
29*           WO = (1.0/(AN*DF*6.28318531))*WO
30*           NW=NW-1
31*           WRITE(6,112) WO,DF, (G(I),PH(I), I = 1,NW)
```

```
      112 FORMAT(//17H DIRECT TRANSFORM,6H W0 = ,2E17.7/10H   MODULUS,
     110H AND PHASE/ (1X,F15.6,F10.2,E15.6,F10.2,E15.6,F10.2,E15.6,F10.2
     2,E15.6,F10.2))
          NW=NW+1
          RETURN
      131 DO 142 I = 1,N
      142  T(I) = W0/2.0
           DO 143 J = 1,NW
           NSG = (PH(J)/360.)*AN
           DO 143 I = 1,N
           IJ = I*J + NSG -N*((I*J + NSG - 1)/N)
      143 T(I) =T(I) + G(J)*CFN(IJ)
           DO 144 I = 1,N
      144 T(I) = 12.5663706*DF*T(I)
          DT = (1.0)/(AN*DF)
          RETURN
          END

          SUBROUTINE DRAW (NTOT, INC, F, SCALE)
     C   NTOT=TOTAL NUMBER OF POINTS IN F.  F IS THE DATA (ONE DIMENSIONAL)
     C   TO BE PLOTTED. INC IS THE SAMPLE INTERVAL FOR PLOTTING F.
     C   SCALE IS THE AMPLITUDE OF ONE FULL SCALE DEFLECTION
          DIMENSION   F(NTOT)
          DATA AA1/1H /,AA2/1H*/,AA3/1H+
          WRITE(6,1011) (I,I=-9,10) , (AA2,M=1,21)
     1011 FORMAT(3X,20I5/2X,22A5)
     10   DO 1501 K = 1, NTOT, INC
          FK = 50.0*((F(K)/SCALE)+0.00001)
          KI = FK/50.
          KK = FK-KI*50.+50.495
      511 FORMAT (1X,110A1)
          WRITE (6,511) AA2, (AA1,I=1,KK),AA2
     1501 CONTINUE
          RETURN
          END
```

```
1*            SUBROUTINE DRAWML (NTOT,INC,F,SCALE,AMAXL,DF)
2*      C    TO BE PLOTTED. INC IS THE SAMPLE INTERVAL FOR PLOTT&NG F.
3*      C    NTOT=TOTAL NUMBER OF POINTS IN F.  F IS THE DATA (ONE DIMENSIONAL)
4*      C SCALE IS THE # OF LOG CYCLES
5*
6*
7*      C SCALE IS THE # OF LOG CYCLES
8*      C  AMAXL IS MAX VALUE OF G(I)
9*            DIMENSION  F(NTOT)
10*           DATA AA1/1H /,AA2/1H*/AA3/1H+
11*           J1=100./SCALE-1
12*           I2=SCALE
13*           WRITE(6,1010) AA2,(((AA3,J=1,J1),AA2),I=1,I2)
14*     1010 FORMAT(11X,115A1)
15*           ALMAX=ALOG10(AMAXL)
16*           MAXF=ALMAX
17*           SCAL=FLOAT(MAXF)+0.5+SIGN(0.5,ALMAX)
18*           DO 1501 K=1,NTOT,INC
19*           FK=100.0*(ALOG10(F(K))-SCAL)/SCALE
20*           KI=FK/100.
21*           KI=-KI+(1.0-SIGN(1.0,FK))/2.0
22*           KK= FK+100.*KI
23*           DDF=DF*K
24*           WRITE(6,511)DDF,AA2,(AA1,I=1,KK),AA2
25*     511   FORMAT(1X,F10.2,110A1)
26*     1501  CONTINUE
27*           RETURN
28*           END
```

```
1*            SUBROUTINE MXSCL(N,A,AMAX)
2*            DIMENSION A(N)
3*            AMAX = 0
4*            DO 26 I = 1,N
5*            IF (ABS(A(I))-AMAX) 26,26,25
6*         25 AMAX = ABS(A(I))
7*         26 CONTINUE
8*            AN = LOG10(AMAX)
9*            IF(AN) 17,18,19
10*        17 NN = AN - 1
11*           GO TO 20
12*        19 NN = AN
13*        20 IA = AMAX/(10.**NN)
14*           IF(IA.LE.2) GO TO 14
15*           IF(IA.LE.5) GO TO 15
16*        16 AMAX = 10.*(10.**NN)
17*        18 RETURN
18*        14 AMAX = 2.*(10.**NN)
19*           RETURN
20*        15 AMAX = 5.*(10.**NN)
21*           RETURN
22*           END

1*            SUBROUTINE DIGI(H,T,N,TI,NDT,DT,F)
2*            DIMENSION H(I),T(I),F(NDT)
3*            PI=3.1415926536
4*            I=0
5*            DO 20 J=1,NDT
6*            TIME=TI + (J-1)*DT
7*         22 IF (T(I+1).GT.TIME) GO TO 20
8*            I=I+1
9*            GO TO 22
10*        20 F(J)=(H(I)+H(I+1))*0.5+(H(I)-H(I+1))*0.5*COS(PI*(TIME-T(I)
11*          *)/(T(I+1)-T(I)))
12*           RETURN
13*           END
```

APPENDIX II

Locations

The locations were chosen in a variety of geologic settings on mostly level areas. This facilatated analysis by eliminating the topographic complications.

Location AT was near the intersection of I-75 and I-285 south of Atlanta, Georgia on a seldom used paved road. The road was built on residual clay in an ultra mafic rock area.

AT4 was also in Atlanta, Georgia. It was on a paved road near Northside Circle and Northside Drive near a mylonite zone.

SR and AR located on Georgia 212 SE of Atlanta, Georgia on Evans Mill Road and monitored a 1971 Toyota Corona Mark II traveling on Lyons Road. Both roads were clay underlain by an undifferentiated granite gneiss.

SR2 was three miles South of Lathonia, Georgia on a massive granite outcrop. The two lane asphalt road was bedded on hard rock as was the geophone.

SR4 was on I-85 0.75 mile north of the McCollum-Sharpsburg exit and 6 mile north of Newnan at an unfinished exit. This station in the Piedmont was on a clay fill underlain by hard rock.

SR5 and AT10 located 0.5 miles south of I-85 on US 29 near Auburn, Alabama. The scene was an asphalt two lane road with a perpendicular dirt driveway for geophone positions. This was in the Coastal Plain.

Also in the Coastal Plain, SR6 and AT11 were on I-85 at the Wire Road exit west of Auburn, Alabama. These like SR5 were underlain by much sediment.

APPENDIX III

SOURCE

Station	Car Type	Speed (mph)	Particle Velocity (cm./s.)
SR	Toyota test car	10	8.00×10^{-5}
		30	1.95×10^{-4}
		40	1.62×10^{-4}
		25	1.23×10^{-4}
		35	1.52×10^{-4}
		20	8.33×10^{-5}
SR2		30	1.53×10^{-5}
		20	1.13×10^{-5}
		65	1.05×10^{-5}
		55	1.24×10^{-5}
		40	1.21×10^{-5}
		60	6.92×10^{-6}
SR5	Chevy	68	2.65×10^{-4}
	Vega	58	2.71×10^{-4}
	Pinto	47	2.84×10^{-4}
	Ford	62	2.39×10^{-4}
	Comet	44	2.33×10^{-4}
	Falcon	49	1.83×10^{-4}
	Chevy	44	1.32×10^{-4}
	Dart	51	2.46×10^{-4}
SR6	Semi	68	1.89×10^{-4}
	Chevy	59	1.26×10^{-4}
	Lincoln	68	1.13×10^{-4}
	Chevy	63	3.72×10^{-4}
	VW Camper	51	1.70×10^{-4}
SR6	VW	69	1.13×10^{-4}
	Volvo	66	6.93×10^{-5}
	Van	83	2.71×10^{-4}
	Honda	53	6.93×10^{-5}
SR4	Semi	44	1.51×10^{-3}
	Pontiac	58	5.99×10^{-4}
	Pontiac	51	5.36×10^{-4}
	Mercury	48	6.30×10^{-4}
	Semi	59	1.89×10^{-3}
	Vega	51	7.56×10^{-4}
	VW	51	4.41×10^{-4}
	Ford	47	7.88×10^{-4}
	Semi (almost)	49	1.64×10^{-3}

APPENDIX III (Continued)

Station	Car Type	Speed (mph)	Particle Velocity (cm./s.)
	Semi	53	4.50×10^{-3}
	Ford	62	6.93×10^{-4}
	Semi	59	4.19×10^{-3}
	Maverick	43	5.67×10^{-4}
	Semi	49	3.09×10^{-3}
	Pick-up	51	7.25×10^{-4}
	Ford	52	5.67×10^{-4}

BIBLIOGRAPHY

1. Akamatu, Kei, On Microseisms in Frequency Range 1 c/s to 200 c/s, Bull. Earthquak Research Inst., Tokyo Univ., v. 39 (1961) pp. 23-75.

2. Brune, James N. and Oliver, Jack, The Seismic Noise of the Earth's Surface, Bull. Seis. Soc. Amer., v. 49 (1959) pp. 349-353.

3. Douze, E.J., Short-Period Seismic Noise, Bull, Seis. Soc. Amer., v. 57 (1967) pp. 55-81.

4. Fix, James E., Ambient Earth Motion in the Period Range from 0.1 to 2560 Sec., Bull. Seis. Soc. Amer., v. 62 (1972) pp. 1753-1760.

5. Franti, G.E., Willis, D.E., and Wilson, J.J., The Spectrum of Seismic Noise, Bull. Seis. Soc. Amer., v. 52 (1962) pp. 113-121.

6. Franti, G.E., The Nature of High-Frequency Earth Noise Spectra, Geophysics, v. 28 No. 4 (1963) pp. 547-562.

7. Kanai, Kiyoshi, T. Tanaka, and K. Osada, "Measurement of Micro-Tremor I to Measurement of Micro-Tremor VII", Bull. Earthquake Research Inst., Tokyo Univ., 1954, I v.32, pp. 199-209, 1957 (II-VII), v. 35, pp. 109-200.

8. Hatherton, T., Microseisms at Scott Base, Geophys. J. of the Roy. Astronomical Soc., v. 3 (1960) p. 381-405.

9. Long, L.T., A Study of Short-Period Microseisms, M.S. Thesis, New Mexico Institute of Mining and Technology, (1964).

10. Long, L.T., Investigation of Seismic Road Noise, Project #A-1357 performed for Greiner Environmental Systems, Inc., Atlanta, Georgia; Engineering Experimental Station, Georgia Institute of Technology, Atlanta, Georgia (1971).

11. Mather, Keith B., Why do Roads Corrugate? Scientific American, Vol. 208, No. 1, (1963) pp. 128-136.

12. Romney, Carl F., Symposium on Microseisms, National Academcy of Sciences, The Geotechnical Corporation (1953) pp. 70.

13. Sanford, Allan R., Carapetian, Ara G. and Long, Leland T., High-Frequency Microseisms from a Known Source, Bull. Seis. Soc. Amer., v. 58 (1968) pp. 325-338.

BIBLIOGRAPHY (Continued)

14. Wilson, C.D.V., The Origins and Nature of Microseisms in the Frequency Range 4 to 100 c/s, Pro., Roy. Soc., v. A217, (1953), pp. 176-188.